Renewable and Sustainable Energy Reviews 109 (2019) 333–348

Contents lists available at ScienceDirect

Renewable and Sustainable Energy Reviews

journal homepage: www.elsevier.com/locate/rser

Improved SuDoKu reconfiguration technique for total-cross-tied PV array to enhance maximum power under partial shading conditions

G. Sai Krishna*, Tukaram Moger

Department of Electrical and Electronics Engineering, National Institute of Technology Karnataka, India

ARTICLE INFO

Keywords:
PV modelling
Partial shading conditions (PSCs)
SuDoKu puzzle pattern
TCT PV array

ABSTRACT

Mismatch losses ignore the performance of individual photovoltaic (PV) modules and cut back most of the power from the PV array. These losses mainly due to partial shading condition (PSC), are caused by the reduction of spacing between PV modules, passing clouds, and near buildings, etc. Several techniques are present in the literature to cut back the partial shading issues. One of the most effective methods is the reconfiguration techniques, namely reconfigure the location of PV modules in PV array so as to distribute partial shading effects and increase the maximum power output. This paper proposes an Improved SuDoKu reconfiguration pattern for 9×9 Total-Cross-Tied (TCT) PV array to enhance maximum power output under partial shading conditions. The main aim of this approach is to arrange the PV modules in TCT array according to the SuDoKu pattern without altering the electrical connections. Further, the performance of the proposed pattern is evaluated with different existing PV array configurations by comparing the Global Maximum Power Point (GMPP), Mismatch Losses (ML), Fill Factor (FF) and Efficiency (η). Based on the results of this paper, it is concluded that the proposed improved SuDoKu PV array arrangement enhances the global maximum power under all shading conditions.

1. Introduction

In the recent years, the renewable energy sources (RES) become more popular and broadly replaced conventional energy sources. Examples of RES are the solar, the wind, the biomass and the geothermal energy sources. Among all, solar energy is the most essential and prerequisite sustainable resource because of its ubiquity and abundance in nature [1,2]. The energy from photovoltaic (PV) arrays, in addition to requiring little Maintenance, is fuel free and pollution free. Also, the PV energy is employed in several scenarios such as: residential buildings, street lights, integration of power systems and rural areas. The efficiency of PV modules is affected by various factors, but one of the most significant issues is partial shadings. Partial shading occurs if the PV modules are shaded in PV array by cause of flying birds, passing clouds and adjacent buildings, etc. Under PSCs, the amount of irradiance received by the shaded module is smaller than that received by the unshaded module. Since the shaded PV module limit the output current of an array, the entire PV system is affected by mismatch losses, that might cause the damage to the PV cells or modules [3,4]. One of the ways to protect the shaded PV modules from the damage is by connecting bypass diodes across the terminals. Insertion of bypass diodes causes multiple steps in I-V and multiple peaks in P-V characteristics of the PV array [5]. Among the multiple peaks, there is only one global peak (GP) which produces the highest maximum power, which is also known as Global Maximum Power Point (GMPP) and rest of all Local Maximum Power Points (LMPPs). The existence of multiple peaks may mislead the maximum power point tracking (MPPT) technique by tracking the LMPPs instead of GMPP; this would add extra power loss to the PV system [6,7].

The power loss as a result of partial shading is dictated by the chosen array configuration, shading pattern and physical location of PV modules in the PV array. However, the effect of PV array configuration shows a severe impact on maximum power output. Therefore, choosing the right configuration is necessary under PSCs. Various PV array configurations are reported in the literature to reduce mismatch losses caused by partial shadings such as “simple-series (SS), parallel (P), series-parallel (SP), total-cross-tied (TCT), bridge-link (BL) and honeycomb (HC) [8,9]. In Ref. [10], the authors have considered three PV array configurations, such as SP, TCT and BL, to evaluate reliability, using a probabilistic approach under mismatch effects due to manufacturing tolerance. This paper indicates that TCT and BL PV array configurations minimize the mismatch losses and increase the reliability as compared to the SP PV array. In Ref. [11], analysis and comparison of different PV array configurations such as “SS, SP, TCT, BL, and HC” under partial shading conditions are presented. During the study, the authors have adopted various parameters to evaluate the

* Corresponding author.
E-mail address: saikrishna240@gmail.com (G. Sai Krishna).

https://doi.org/10.1016/j.rser.2019.04.037
Received 29 December 2018; Received in revised form 10 April 2019; Accepted 11 April 2019

Nomenclature

$V_{cell}/V_m/V_a$	PV cell/module/array voltage (V)
$I_{cell}/I_m/I_a$	PV cell/module/array current(A)
I_{Lcell}	light generated current in PV cell
I_d	diode current
I_{sh}	Shunt current
T_c	PV module operating temperature
T_{STC}	Standard operating temperature at 298.15 K
I_o	saturation current of the diode
R_s	&R_{sh} series and shunt resistance of the PV cell
a	Ideality factor
k	Boltzmann's constant 1.3805× 10^{-23} J/K
q	Electron charge 1.6× 10^{-19} C
G	Actual Irradiance of the PV module
G_o	Standard PV module irradiance at 1000 W/m^2
N_{pv}	Number of PV modules
m	Number of rows
η	Efficiency

Abbreviations

GMPP	Global Maximum Power Point
ML	Mismatch Losses
FF	Fill factor
TCT	Total-Cross-Tied
SP	Series-Parallel
BL	Bridge-Link
HC	Honey-Comb

performance of each configuration. The obtained result shows that the TCT PV array is defeating the mismatch losses as compared to other configurations. In Ref. [12], modelling and simulation of "SS, P, SP, TCT, BL and HC" PV array configurations under various partial shading conditions is presented. In this paper, the performance analysis is carried out for each configuration by considered the GMPP, ML, FF, and efficiency. This paper is assuring that the TCT PV array is enhancing the maximum global power as compared to the other PV array configurations. Therefore, according to the literature, the TCT PV array is producing the highest maximum power as compared to the existing configurations under PSCs. However, a critical issue with the TCT configuration is that if the number of PV modules are shaded in a row, that limits the output current of an array [13]. However, to unravel this issue, many authors have been proposed reconfiguration techniques for TCT array to distribute shading effects from one row into different rows uniformly, to scale back mismatch losses under PSCs [14,15].

According to the literature, the reconfiguration techniques are classified into dynamic and static techniques. In dynamic techniques, the PV modules are reconfigured dynamically within the PV array to increase maximum power output under PSCs. In Refs. [16,17], an Electrical Array Reconfiguration (EAR) controller is developed to change the connections between among the PV modules based on irradiance levels for providing input current to the motor. This approach is also employed for an electric car to improve the performance at different driving states such as initial, acceleration, and high-speed [18]. In this paper, the fuzzy logic controller is applied to choose the EAR automatically according to driving states. In Refs. [19,20], a PV system with an electrical array reconfiguration controlled by irradiance equalization algorithm (IE) has been presented. The EAR PV system act as a static part to satisfy the inverter constraints and reconfigurable part; each PV module can connect with any of the rows in the array based on the proposed algorithm. In Ref. [21], proposed an optimal reconfiguration approach to reduce irradiance mismatch index (IMI). The main aim of this reconfiguration is to shift the location of shaded PV modules from one place to different places within the PV array to improve maximum power output under PSCs. In Ref. [22], a new adaptive PV cell array technique is proposed to reduce PSCs. It consists of a fixed part, an adaptive part, and a switching matrix. In this technique, the switching matrix plays a crucial role to connect adaptive PV cells into the fixed cells in order to compensate irradiance drop in each row [23]. Many authors in the literature have discussed dynamic reconfiguration techniques, which are presented in Table .1. According to the literature, a dynamic reconfiguration technique requires the sensors to identify the shading and faulty conditions, reconfiguration algorithm to optimize the maximum power and switching matrix to connect switching between the PV modules. All these tasks increase the cost of a dynamic technique, as well as the configuration of the system becomes complex [14,24,25].

A static technique utilizes a fixed interconnection scheme, namely, the physical location of the PV modules is changed in the PV array without altering electrical connections. This technique does not require any sensors, reconfiguration algorithm or switching matrix, in opposition to the dynamic technique case. However, it needs an effective reconfigurable pattern for arranging the location of PV modules so as to distribute shading effects over the array. In Ref. [38], the authors proposed a novel interconnection scheme to distribute partial shading effects over the array. The proposed scheme is implemented on a 3×3 PV array, and the result shows that the proposed scheme enhances the global maximum power as compared to the SP, TCT and BL PV array configurations. In Ref. [39], a magic-square arrangement is proposed for TCT PV array to increase maximum power output under PSCs. In this paper, various existing PV array configurations are considered and compared to the proposed arrangement. The obtained result shows that the magic-square arrangement reduces the mismatch losses as compared to other configurations under all shading cases. Consequently, the same authors [40] introduced two non-symmetrical PV array arrangements for TCT PV array to distribute PSCs. This paper indicates that the proposed arrangements are diminishing the mismatch loss and increasing the fill-factor. In Ref. [41], the authors proposed a SuDoKu arrangement for TCT PV array to enhance maximum power under PSCs. In this approach, the physical location of PV modules in TCT array is adjusted according to SuDoKu arrangement to distribute PSCs. Similarly, an optimal SuDoKu arrangement is developed to distribute partial shading effects [42]. During this study, it is observed that the optimal SuDoKu arrangement is characterized by superior performance than the SuDoKu [41]. Still, many reconfigurable patterns have been reported in the literature, which are presented in Table .2. However, according to Refs. [41,42] few shortcomings are found; (i) The first column of the reconfigurable patterns remains unaltered (see Fig. 1). It means that if the shadow falls on the left side of the array it will remain undistributed; this leads to a reduction in power output and also causes multiple peaks in P-V characteristics. (ii) These patterns have issues with repeated row-number modules in the diagonal (For example, 9^{th} row of the PV modules 91,97,96 are connected in diagonal shown in Fig. 1, highlighted). As a result, the shaded PV modules in the same row (i.e., after shading dispersion) are increased and the output current of the array is reduced. Therefore, to overcome these problems, this paper develops an improved SuDoKu arrangement for 9×9 TCT array to enhance maximum power output under PSCs. In this approach, the physical location of PV modules in the TCT array is adjusted according to the improved SuDoKu arrangement without altering the electrical connections. It follows that, the shading effects in the same row distribute over the PV array. Moreover, the performance of the proposed arrangement is evaluated with "SP, TCT, BL, HC, SuDoKu [41] and optimal SuDoKu" [42] PV array configurations by comparing the GMPP, ML (%), FF(%) and η(%) under various shading conditions using

Table 1
Resume of dynamic PV array reconfiguration approach with the TCT topology in terms of: Reconfiguration strategy, control algorithm, number of switches, acquired parameters, applications and remarks.

Author	Reconfiguration Strategy	Control Algorithm	Required Switches	Acquired Parameters	Applications	Remarks
[19]	IE	Refer [19]	$2N_{pv}$m-throws	current,voltage	PV-Grid	developed static and dynamic part
[21]	IE	Branch and Bound	$m.\ n_R$ double pole m-throw	irradiance	PV farm	proposed fixed part along with adaptive part
[26]	IE	Deterministic and Random search	$(N_{pv})_{DPST} + m_{SPST}$	irradiance	NS	support a row with non-symmetrical number of modules
[27]	IE	Best worst sorting	$N_{pv}(m^2 - m)_{spst}$	current,voltage	NS	support a row with non-symmetrical number of modules
[28]	Dynamic PV array	refer [28]	15-SPST,5-DPDT	voltage,irradiance	DC-loads	Dynamic PV array structure is developed for DC-loads
[22]	Adaptive bank	Bubble-sort,Model based	$(2N_{AB}N_{pv})_{spst}$	voltage,temperature	R-Load	developed fixed part along with the adaptive part
[29]	Adaptive bank	Neural Network	NS	temperature,current	R-Load	developed fixed part along with the adaptive part
[24]	Adaptive bank	Scanning algorithm	$2.\ m.\ m$	current	R-Load	the proposed algorithm scans the output currents of a PV modules
[30]	Adaptive bank	Image process,canny algorithm	NS	current,voltage	R-Load	based on the shadings fixed part is to connect with adaptive part
[31]	Adaptive Reconfiguration	Fuzzy and Fitter Estimator	$n + 6$	current,voltage	R-Load	adaptive part connects the PV modules automatically
[32]	Adaptive bank	Fuzzy control	NS	current	R-Load	developed fixed part along with adaptive part
[33]	IE	Refer [33]	NS	irradiance	NS	support a row with non-symmetrical number of modules
[34]	IE	DP and SC	NS	irradiance,current	NS	support a row with non-symmetrical number of modules
[35]	IE	Reconfiguration algorithm	NS	irradiance	NS	support a row with non-symmetrical number of modules
[36]	IE	Greedy algorithm	NS	irradiance	NS	the proposed algorithm connects the PV modules based on shadings
[37]	Adaptive topology	Refer [37]	3-switches for each module	current, voltage	R-Load	adaptive part connects the modules automatically

*NS; Not Specified.

Table 2
Resume of static PV array reconfiguration approach with the TCT topology in terms of: Reconfigurable pattern, Array size, study of shading patterns, the complexity of implementation, type of PV array configuration is chosen and remarks.

Author	Reconfigurable Pattern	Implemented Array Size	Types of Shadings	Complexity	Configurations	Remarks
[38]	Renumbering pattern	5×5, 6×6	SW,LW,SN,LN	High	TCT	PV modules are renumbered before the connection
[43]	Futoshiki puzzle pattern	5×5	SW,LW,SN,LN	Medium	TCT	proposed Futoshiki arrangement for TCT
[41]	Su-Do-Ku puzzle	9×9	SW,LW,SN,LN	High	TCT	developed Su-Do-Ku puzzle arrangement for TCT
[40]	Non-symmetrical patterns	5×4	vertical, horizontal, diagonal	High	TCT	proposed non-symmetrical arrangement for TCT
[39]	Magic Square Puzzle	4×4	vertical, horizontal, diagonal	High	TCT	proposed a magic-square puzzle arrangement for TCT
[44]	Latin Square Puzzle	4×4	vertical, horizontal, diagonal	High	TCT	developed Latin-square arrangement for TCT
[45]	Optimal Su-Do-Ku	9×9	Horizontal, diagonal, bottom left & right	High	TCT	an Optimal Su-Do-Ku arrangement is proposed
[46]	static shade tolerant scheme	3×3,5×5	Horizontal,vertical,etc	High	TCT	PV modules are renumbered before the connection
[47]	Shadow Dispersion Scheme	7×7	SW,LN,center, one module patterns	High	TCT	PV modules are renumbered before the connection
[48]	Zig-Zag scheme	4×4	Double row, single row,corner,oblique	High	TCT	proposed a Zig-Zag arrangement for TCT
[49]	Adjacent shifting pattern	9×9	SW,LW,SN, LN	High	TCT	PV modules adjacent shifting arrangement for TCT
[50]	dominance square pattern	5×5	SW,LW,SN, LN	High	TCT	developed dominance square arrangement for TCT

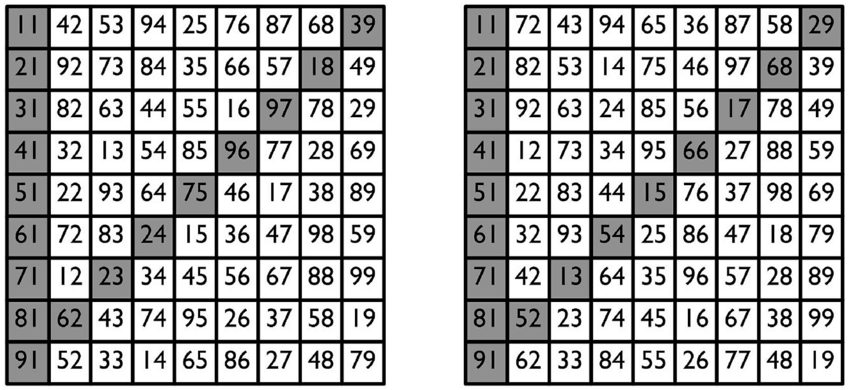

(a) SuDoKu pattern [41] (b) Optimal SuDoKu pattern [42]

Fig. 1. SuDoKu and optimal SuDoKu pattern.

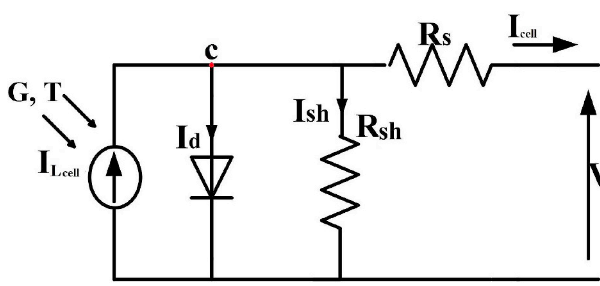

Fig. 2. Equivalent circuit of single diode PV cell model.

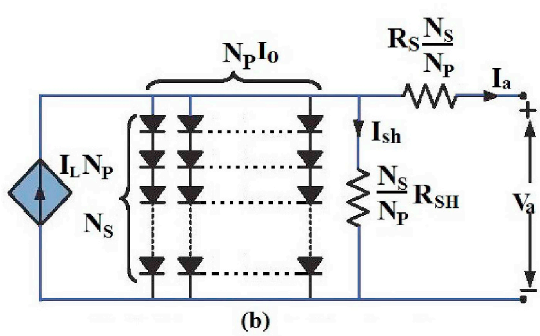

Fig. 3. PV array composed of $N_S \times N_P$

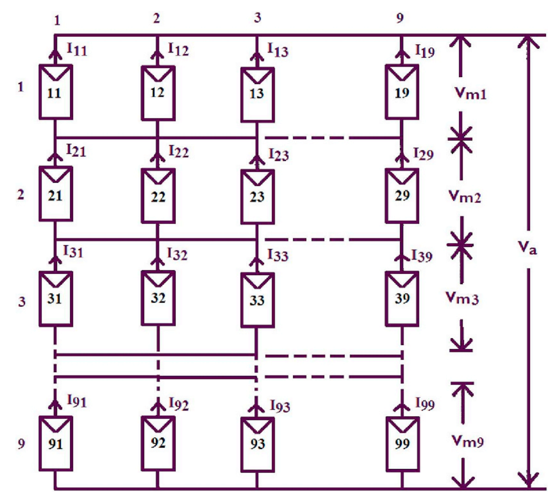

Fig. 4. 9 × 9 TCT PV array Configuration.

Table 3
PV module data sheet parameters [40].

Parameters	Ratings
Rated Power (P_{mpp})	170 W
Open-Circuit Voltage (V_{oc})	44.2 V
Short-Circuit Current (I_{sc})	5.2 amps
Current at Maximum Power (I_{mp})	4.75 amps
Voltage at Maximum Power (V_{mp})	35.8 V
Number of Cells	72
PV Module Area	62.2inc×31.9 inc

MATLAB-SIMULINK.

The following Sections of this paper is organized as follows: Section 2, presents detailed modelling of PV array. In Section 3, formation of an Improved SuDoKu puzzle and pattern arrangement are discussed. In Section 3.1, the description of partial shading conditions considered in this paper are reported. In Section 4, results and discussions of improved SuDoKu arrangement under different shading conditions are explained in detailed. The conclusion is presented in Section 5.

2. Mathematical modelling of PV array

Modelling is the first step for analyzing the behavior of PV systems. In fact, good and accurate mathematical models are necessary to achieve the operation at an optimum point under partial shadings [51]. The modelling of PV arrays starts with the mathematical model of a single PV cell. Many PV cell models have been reported in the literature [52]. Two of them are the one diode PV cell and the two diode PV cell models. As it is mentioned in the literature, the one diode PV cell model requires less computational efforts as compared to the two diode model [53]. Hence, many researchers are widely using one diode PV cell model because it is very easy to model as compared to the other models. The equivalent circuit of single diode PV cell model is shown in Fig. 2. The modelling equations are as follows;

By applying KCL to node ‘c’ in Fig. 2, I_{cell} can be written as,

$$I_{cell} = I_{Lcell} - I_d - I_{sh} \tag{1}$$

The general representation of I-V characteristics for the PV cell is given by,

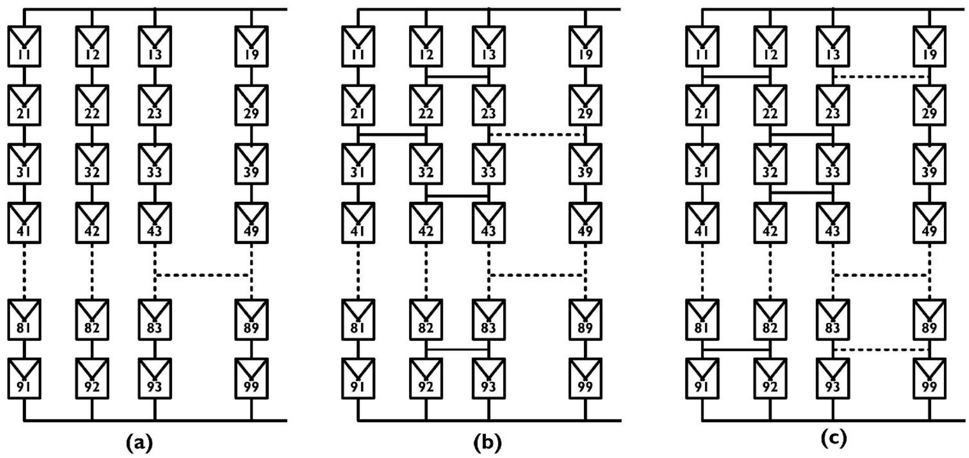

Fig. 5. PV array configurations: (a) Series-Parallel (SP), (b)Bridge-Link (BL), (c) Honey-Comb (HC).

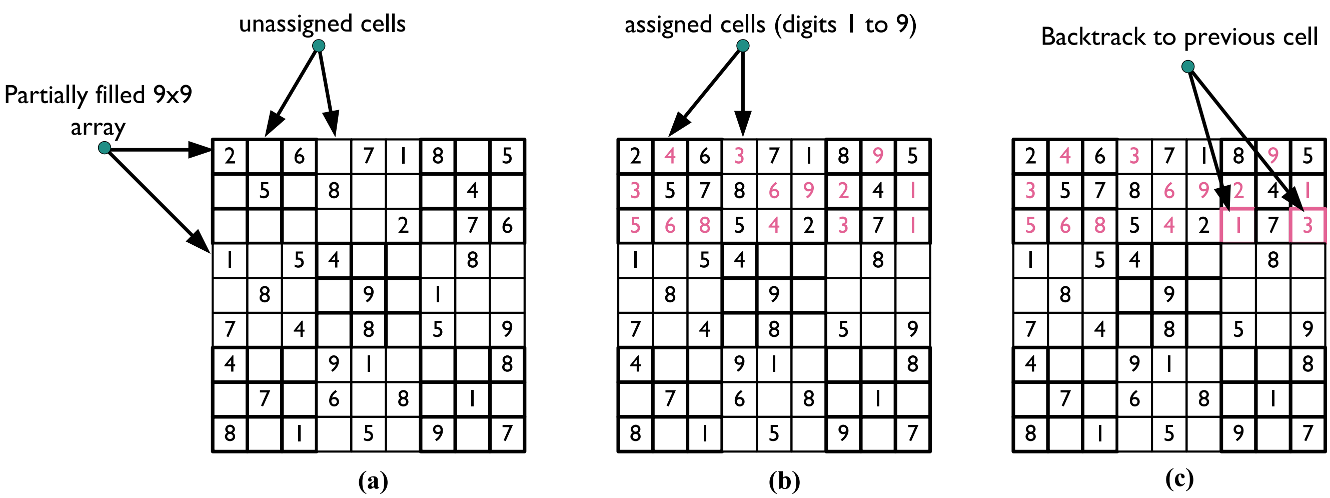

Fig. 6. Illustration of proposed algorithm (a)partially filled 9 × 9 array(b)filling digits in the unassigned cells (i.e., pink colour), and (c) digit 1 already exists in the 9th column so that exchange the cells using backtracking. (For interpretation of the references to colour in this figure legend, the reader is referred to the Web version of this article.)

$$I_{cell} = I_{Lcell} - I_o\left[exp\left\{\frac{q(V_{cell} + I_{cell}R_s)}{kaT_c} - 1\right\}\right] - \frac{(V_{cell} + I_{cell}R_s)}{R_{sh}} \tag{2}$$

To form a PV module is by connecting the number of solar cells in series (n_s). The mathematical representation of I-V characteristics for the PV module is given in Eq. (3),

$$I_m = I_L - I_o\left[exp\left\{\frac{q(V_m + I_mR_S)}{n_skaT_c} - 1\right\}\right] - \frac{(V_m + I_mR_S)}{R_{SH}} \tag{3}$$

where R_S and R_{SH} are series and shunt resistance of the PV module and I_L is light generated current of the module, which can be represented as,

$$I_L = \frac{G}{G_o}\left[I_{LSTC} + K_{isc}(T_c - T_{STC})\right] \tag{4}$$

where K_{isc} is short-circuit co-efficient of the PV module, I_{LSTC} is the light generated current at standard test condition (STC).

Eq. (3) is a transcendental equation and by using this, one can find the output current of a PV module. However, the use of Eq. (3) is not restricted to one PV module; it can also be used to describe many modules connected in series to form a string. Such strings are connected in parallel to form a PV array is shown in Fig. 3. The simplified mathematical equation of I-V characteristics for the PV array is presented in Ref. [54]and it is given by

$$I_a = N_P.\, I_L - N_P.\, I_o\left[exp\left\{\frac{q\left(V_a + \frac{N_S}{N_P}I_aR_S\right)}{N_SkaT_c} - 1\right\}\right] - \frac{\left(V_a + \frac{N_S}{N_P}I_aR_S\right)}{\frac{N_S}{N_P}R_{SH}} \tag{5}$$

where N_S and N_P are the number of modules connected in series and parallel of the PV array, respectively. The above set of equations is used to model the PV array and to simulate I-V and P-V characteristics with

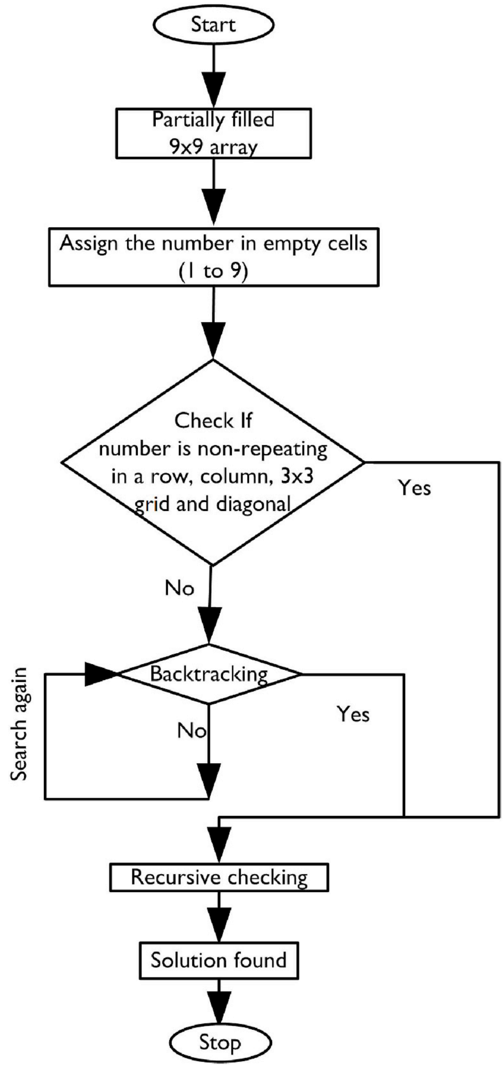

Fig. 7. Flowchart of the proposed algorithm for developing the puzzle.

the help of data sheet parameters presented in Table 3.

2.1. Total-cross-tied PV array configuration

As it is mentioned in section 1, TCT PV array reduces mismatch losses as compared to the other configurations. In TCT, first PV modules are connected in parallel to make tiers (rows), and then all tiers are combined in series to form a string. The general layout of TCT configuration is shown in Fig. 4. It consists of 81 PV modules, arranged into nine rows and nine columns. In each row nine PV modules are connected in parallel. The voltage across each row is same as the open-circuit voltage of a single PV module, and the overall output voltage of the array is equal to the sum of row voltages. The output voltage of a TCT array can be obtained by applying Kirchhoff's Voltage Law (KVL) to the network in Fig. 4,

$$V_a = \sum_{p=1}^{9} V_{mp} \tag{6}$$

where V_{mp} refers to the maximum voltage at the p^{th} row. The PV array current is equal to the sum of all currents of the modules which are connected in parallel in a row; this can be calculated by applying KCL to each node in Fig. 4, the output current of an array (I_a) can be written as;

$$I_a = \sum_{q=1}^{9} (I_{pq} - I_{(p+1)q}) = 0 \quad p = 1,2,3, \ \ldots 9 \tag{7}$$

where p and q are the number of rows and columns of the PV array. The other 9×9 SP, BL and HC PV array configurations are shown in Fig. 5.

3. Improved SuDoKu Puzzle and Pattern arrangement

9×9 Improved SuDoKu is a logic-based number placement puzzle. It consists of nine 3×3 sub-array matrices. The formation of this logic puzzle is based on the Backtracking method. Backtracking is an algorithm for finding solutions to some computational problems, notably constraints satisfaction problems. The constraint of this problem is to place the digits 1 to 9 in 9×9 array so that each row, each column, each 3×3 sub array and diagonal contains the same number only once. The proposed algorithm works as follows. This algorithm mainly is constituted of four consecutive steps to achieve the solution. (i) Choose partially filled 9×9 array as shown in Fig. 6(a). (ii) Try to fill each unassigned cell with the digits from 1 to 9 (see Fig. 6(b)). (iii) If the assigned digit satisfies the condition (i.e., the aforementioned constraint), then try to fill each unassigned cell by performing recursive checking until build the solution (see Fig. 6(b)). (iv) Otherwise, the

2	4	6	3	7	1	8	9	5
3	5	7	8	6	9	2	4	1
9	1	8	5	4	2	3	7	6
1	9	5	4	2	6	7	8	3
6	8	3	7	9	5	1	2	4
7	2	4	1	8	3	5	6	9
4	3	2	9	1	7	6	5	8
5	7	9	6	3	8	4	1	2
8	6	1	2	5	4	9	3	7

(a) Improved SuDoKu Puzzle

21	42	63	34	75	16	87	98	59
31	52	73	84	65	96	27	48	19
91	12	83	54	45	26	37	78	69
11	92	53	44	25	66	77	88	39
61	82	33	74	95	56	17	28	49
71	22	43	14	85	36	57	68	99
41	32	23	94	15	76	67	58	89
51	72	93	64	35	86	47	18	29
81	62	13	24	55	46	97	38	79

(b) Pattern arrangement

Fig. 8. 9×9 Improved SuDoKu Puzzle and Pattern arrangement.

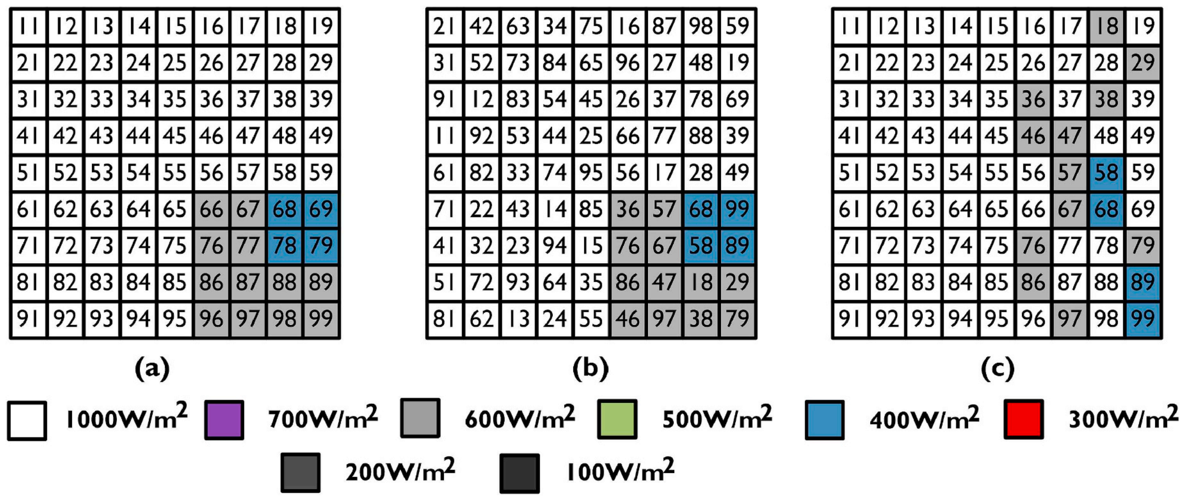

Fig. 9. Group-I shading; (a) TCT PV array arrangement, (b) Improved SuDoKu arrangement, (c) Shading dispersion of improved SuDoKu arrangement.

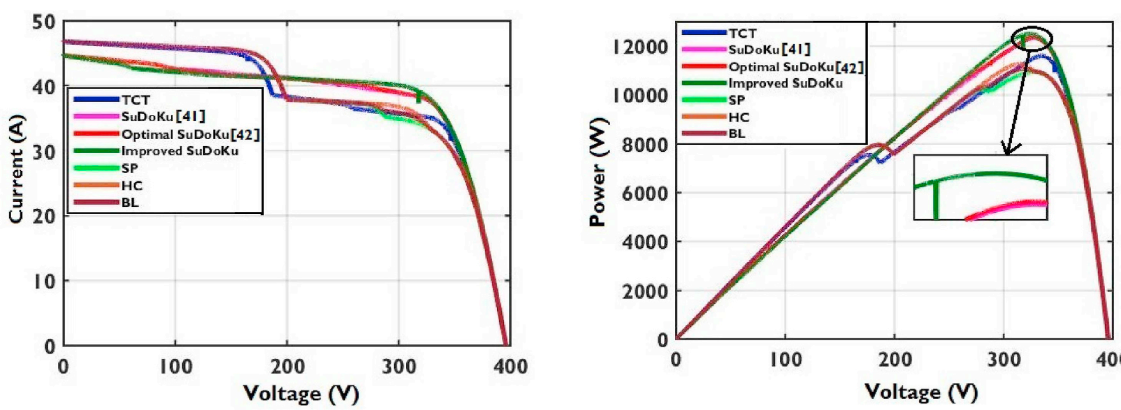

(a) I-V characteristics

(b) P-V characteristics

Fig. 10. Simulation for Group-I shading condition.

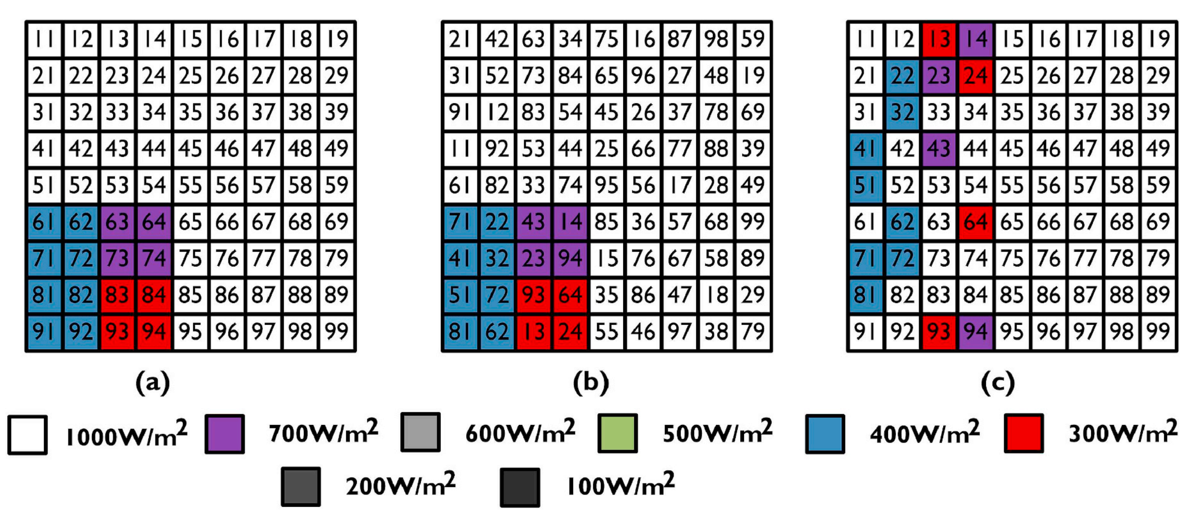

Fig. 11. Group-II shading; (a) TCT PV array arrangement, (b) Improved SuDoKu arrangement, (c) Shading dispersion of improved SuDoKu arrangement.

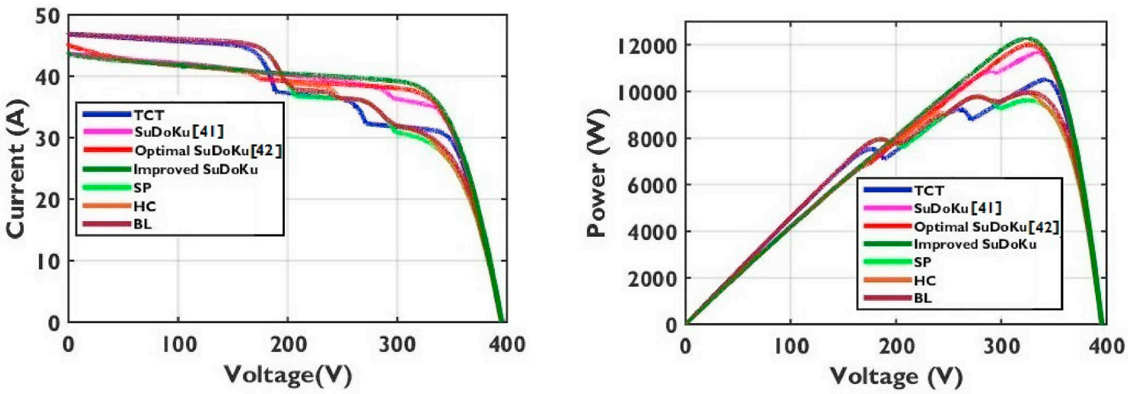

(a) I-V characteristics (b) P-V characteristics

Fig. 12. Simulation for Group-II shading condition.

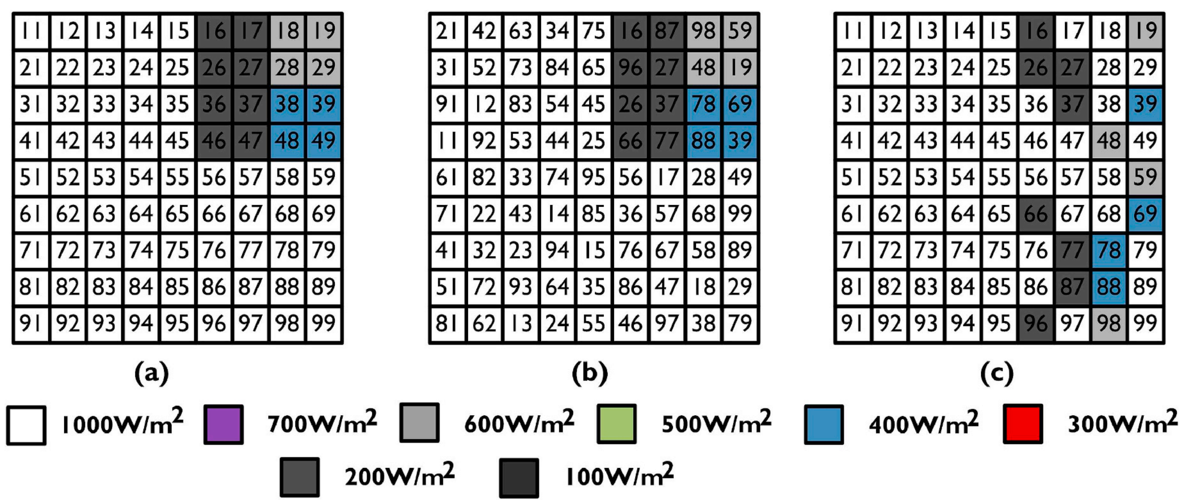

Fig. 13. Group-III shading; (a) TCT PV array arrangement, (b) Improved SuDoKu arrangement, (c) Shading dispersion of improved SuDoKu arrangement.

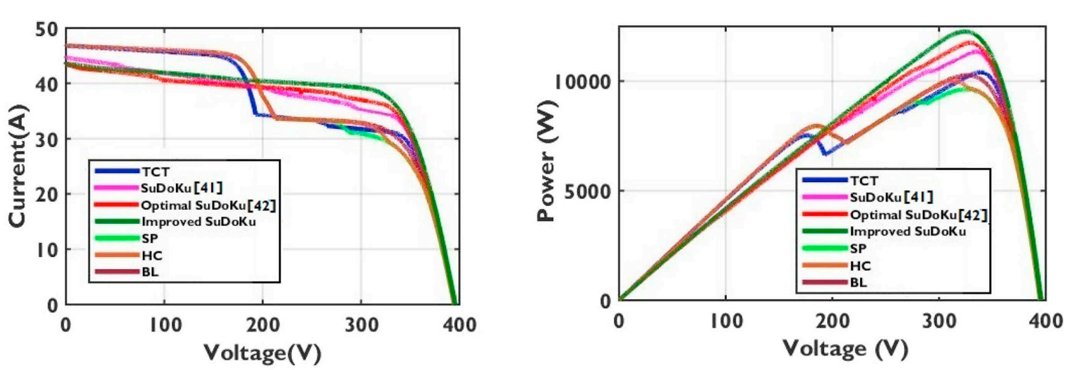

(a) I-V characteristics (b) P-V characteristics

Fig. 14. Simulation for Group-III shading condition.

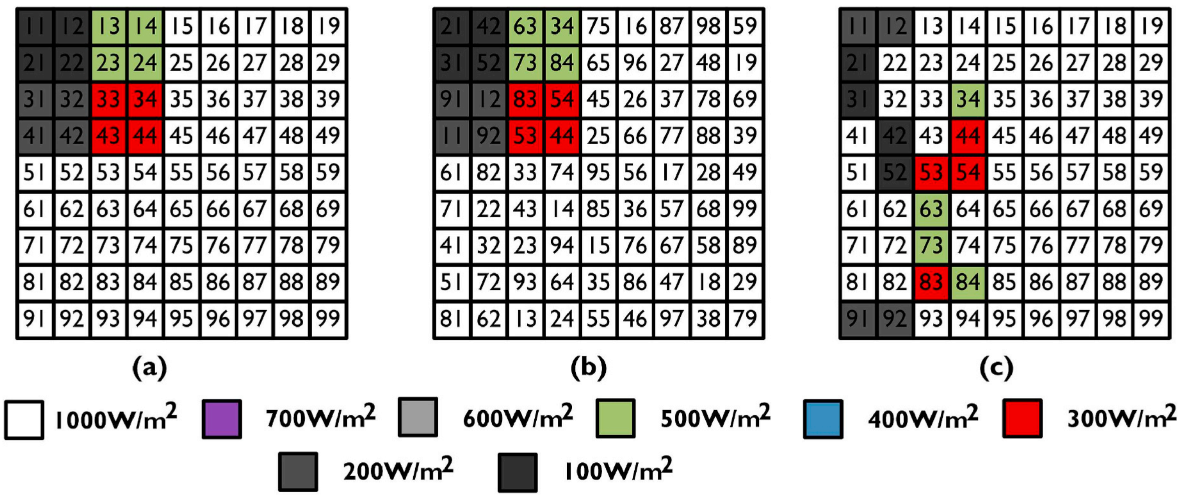

Fig. 15. Group-IV shading; (a) TCT PV array arrangement, (b) Improved SuDoKu arrangement, (c) Shading dispersion of improved SuDoKu arrangement.

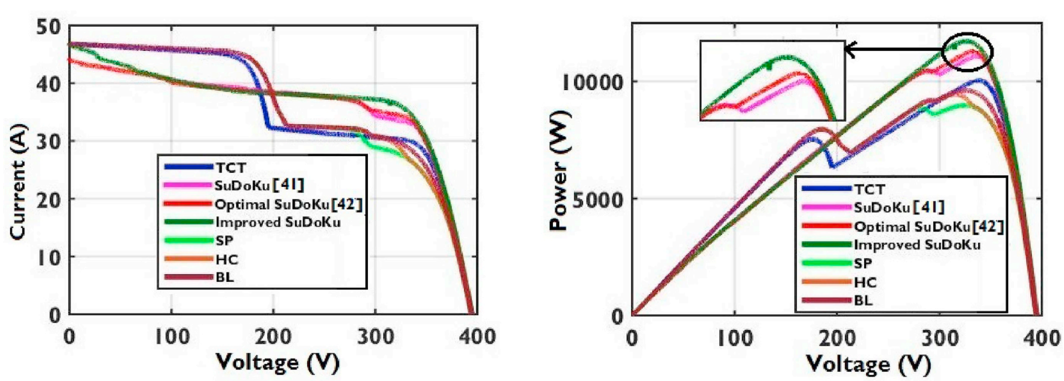

(a) I-V characteristics (b) P-V characteristics

Fig. 16. Simulation for Group-IV shading condition.

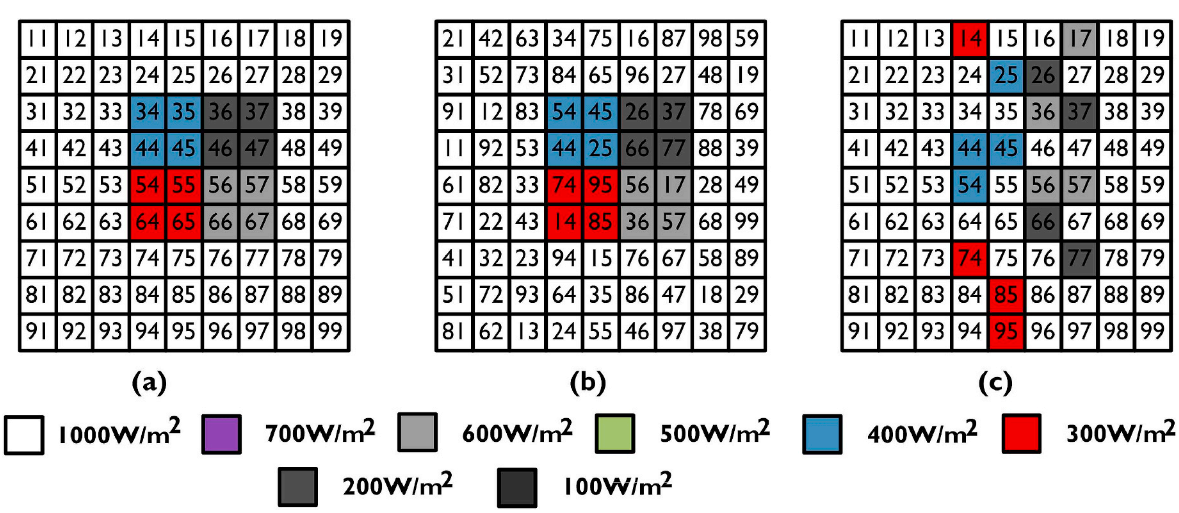

Fig. 17. Group-V shading; (a) TCT PV array arrangement, (b) Improved SuDoKu arrangement, (c) Shading dispersion of improved SuDoKu arrangement.

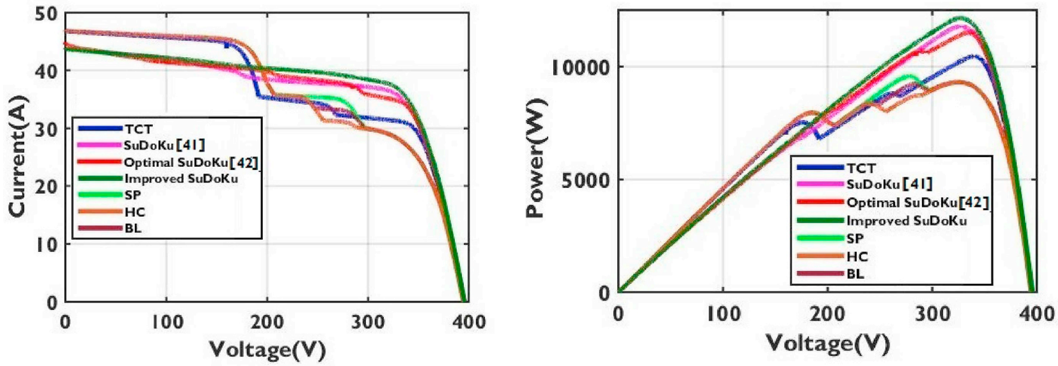

(a) I-V characteristics (b) P-V characteristics

Fig. 18. Simulation for Group-V shading condition.

backtracking algorithm takes place to exchange the assigned cells (see Fig. 6(c)), and tracks the final solution. The flowchart of proposed algorithm is shown in Fig. 7, and the pseudo code is as follows.

Algorithm 1
Pseudo code.

```
Initialize ← SolveSudoku(int grid[N][N])
  If there is no unassigned location
loop If (FindUnassignedLocation(grid, row, col)); return true
  Consider digits 1 to 9
  for (int num = 1; num ≤ 9; num++); return true
  If looks promising
  if (isSafe (grid, row, col, num))
  Make tentative assignment
  If (grid[row][col] = num);return, if success
  if (SolveSudoku (grid)) return true;
end loop
  failure, try again
  grid[row][col] = Unassigned;return false
this triggers backtracking
```

The speciality of this puzzle is that by adding any numbers in a row, column, diagonal and 3×3 sub-array 45 is returned as a result. The developed improved SuDoKu puzzle and pattern arrangement are shown in Fig. 8(a) and (b) respectively. In pattern arrangement, the first digit in the box contains logic number and the second digit refers to a column. The improved SuDoKu arrangement is applied to the TCT PV array by changing the physical location of PV modules without altering the electrical connections. It means that the module number 42 is located at the fourth row-second column of the TCT PV array, but it is physically shifted to the first row-second column in improved SuDoKu arrangement (see Fig. 8(b)) without altering the electrical connections. Similarly, all PV modules in the TCT PV array are arranged according to the improved SuDoKu manner. This enables to distribute the shaded PV modules from the same row into different rows uniformly over the PV array. Therefore, the power output of the PV array is enhanced for the same shading condition.

3.1. Discerption of PSCs

In this article, different partial shading conditions are considered to verify the proposed improved SuDoKu arrangement. They are divided into Group-I, Group-II, Group-III, Group-IV and Group-V and they are shown in Figs. 9, 11, 13, 15 and 17 respectively. In each group, the 4×4 sub-array matrix is subjected to partial shading over 9×9 PV array with different irradiance levels.

3.2. Performance parameters under PSCs

In this paper, four main parameters are considered such as GMPP, mismatch losses (%), fill-factor (%) and efficiency (%) to evaluate the performance of proposed arrangement on 9×9 array under different shading conditions.

3.2.1. Fill factor

Fill factor (FF) measures the area of the PV module or array. FF is depends on the open-circuit voltage (V_{oc}), short-circuit current (I_{sc}), maximum power at voltage (V_{mp}) and maximum power at current (I_{mp}). The FF can be determined as,

$$FF\,(\%) = \frac{Power\ at\ GMPP}{V_{oc}.\ I_{sc}} \tag{8}$$

3.2.2. Mismatch losses

Mismatch loss is the difference between maximum power under uniform irradiance (MPP_{uni}) and the global maximum power under PSCs ($GMPP_{PSCs}$). Mismatch loss can be determined as:

$$ML\,(\%) = \frac{MPP_{uni} - GMPP_{PSCs}}{GMPP_{PSCs}} \tag{9}$$

3.2.3. Efficiency

Efficiency is the ratio between the maximum available power output and the solar input. Efficiency can be calculated by,

$$Efficiency\,(\eta) = \frac{Power\ at\ GMPP}{P_{in}} \tag{10}$$

where P_{in} is the solar irradiance that falls on the PV array.

4. Results and discussions

In this article, an improved SuDoKu arrangement is proposed for TCT PV array to enhance the maximum power output under different

Table 4
Location of GMPP for TCT, SuDoKu [41], Optimal SuDoKu [42] and Improved SuDoKu PV array arrangements under group-I shading condition.

TCT arrangement				SuDoKu arrangement [41]				Optimal SuDoKu arrangement [42]				Improved SuDoKu arrangement			
Row bypassed	currents (I_a)	voltages (V_a)	power (P_a)	Row bypassed	currents (I_a)	voltages (V_a)	power (P_a)	Row bypassed	currents (I_a)	voltages (V_a)	power (P_a)	Row bypassed	currents (I_a)	voltages (V_a)	power (P_a)
$Irow_9$	$7.4I_m$	$7V_m$	$51.8V_m\cdot I_m$	$Irow_9$	$7.8I_m$	$8V_m$	$62.4V_m\cdot I_m$	$Irow_9$	$8.2I_m$	$5V_m$	$41V_m\cdot I_m$	$Irow_9$	$8I_m$	$9V_m$	$72V_m\cdot I_m$
$Irow_8$	$7.4I_m$	–	–	$Irow_8$	$8I_m$	$7V_m$	$56V_m\cdot I_m$	$Irow_8$	$8I_m$	$8V_m$	$64V_m\cdot I_m$	$Irow_8$	$8I_m$	–	–
$Irow_7$	$7I_m$	$9V_m$	**$63V_m\cdot I_m$**	$Irow_7$	$8.6I_m$	$3V_m$	$25.8V_m\cdot I_m$	$Irow_7$	$8I_m$	–	–	$Irow_7$	$8.2I_m$	$5V_m$	$41V_m\cdot I_m$
$Irow_6$	$7I_m$	–	–	$Irow_6$	$8.6I_m$	–	–	$Irow_6$	$8.6I_m$	$3V_m$	$25.8V_m\cdot I_m$	$Irow_6$	$8I_m$	$9V_m$	**$72V_m\cdot I_m$**
$Irow_5$	$9I_m$	$5V_m$	$45V_m\cdot I_m$	$Irow_5$	$7.3I_m$	$9V_m$	**$68.4V_m\cdot I_m$**	$Irow_5$	$8.6I_m$	–	–	$Irow_5$	$8I_m$	–	–
$Irow_4$	$9I_m$	–	–	$Irow_4$	$8.2I_m$	$6V_m$	$49.2V_m\cdot I_m$	$Irow_4$	$8.2I_m$	$5V_m$	$41V_m\cdot I_m$	$Irow_4$	$8.2I_m$	$5V_m$	$41V_m\cdot I_m$
$Irow_3$	$9I_m$	–	–	$Irow_3$	$8.2I_m$	–	–	$Irow_3$	$8.6I_m$	$3V_m$	$25.8V_m\cdot I_m$	$Irow_3$	$8.2I_m$	–	–
$Irow_2$	$9I_m$	–	–	$Irow_2$	$8.2I_m$	–	–	$Irow_2$	$8I_m$	$8V_m$	$64V_m\cdot I_m$	$Irow_2$	$8.6I_m$	$2V_m$	$17.2V_m\cdot I_m$
$Irow_1$	$9I_m$	–	–	$Irow_1$	$8.6I_m$	$3V_m$	$25.8V_m\cdot I_m$	$Irow_1$	$7.6I_m$	$9V_m$	**$68.4V_m\cdot I_m$**	$Irow_1$	$8.6I_m$	–	–

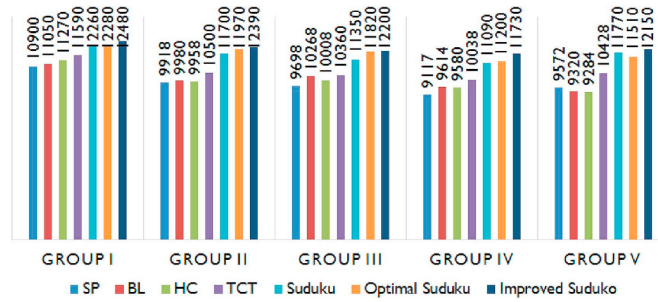

Fig. 19. GMPP for PV array configurations under all shading conditions.

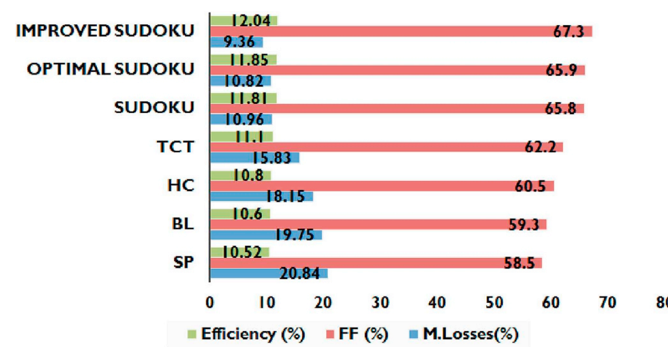

Fig. 20. Mismatch loss, fill factor and efficiency for Group-I shading condition.

shading conditions. Each shading condition, the location of global maximum power point (GMPP) are calculated for TCT, SuDoKu [41], optimal SuDoKu [42] and improved SuDoKu arrangements and validated using Matlab/Simulink. Comparisons are performed also with the SP, BL and HC PV array configurations by evaluating the GMPP, ML (%), FF(%) and η(%).

Group-I Shading: In group-I, the bottom of right corner 4 × 4 sub-array matrix is subjected to partial shading with different irradiance levels as shown in Fig. 9(a). In this condition, the location of GMPP for TCT, improved SuDoKu, SuDoKu and optimal SuDoKu PV array arrangements are calculated by theoretically as follows.

Location of GMPP for TCT arrangement:To find the location of GMPP, it is necessary to calculate the current generated by each row of the PV array.

In group-I shading, all PV modules in *row*1 are receiving 1000 W/m^2 irradiance is shown in Fig. 9(a).

$$I_{row1} = B_{11}I_{11} + B_{12}I_{12} + B_{13}I_{13} + B_{14}I_{14} + - +B_{19}I_{19} \tag{11}$$

$B_{11} = \frac{G_{11}}{G_o} = 1$; where G_{11} is solar irradiance falls on the 11th module of the TCT arrangement and I_{11} is current generated by the PV module. Assume that the current generated by each module at Standard Test Condition (STC) is I_m.Therefore, the current generated by the *row*1 is,

$$I_{row1} = 9 \times I_m \tag{12}$$

All PV modules in *row*2, *row*3, *row*4 and *row*5 are receiving uniform irradiance 1000 W/m^2. So that, the current generated by these rows,

$$I_{row2} = I_{row3} = I_{row4} = I_{row5} = 9I_m \tag{13}$$

In *row*6 and *row*7, first five PV modules are receiving 1000 W/m^2

Table 5
Location of GMPP for TCT, SuDoKu [41], Optimal SuDoKu [42] and Improved SuDoKu PV array arrangements under group-II shading condition.

TCT arrangement				SuDoKu arrangement [41]				Optimal SuDoKu arrangement [42]				Improved SuDoKu arrangement			
Row bypassed	currents (I_a)	voltages (V_a)	power (P_a)	Row bypassed	currents (I_a)	voltages (V_a)	power (P_a)	Row bypassed	currents (I_a)	voltages (V_a)	power (P_a)	Row bypassed	currents (I_a)	voltages (V_a)	power (P_a)
$Irow_9$	$6.4I_m$	$9V_m$	**$57.6V_m \cdot I_m$**	$Irow_9$	$8.4I_m$	$3V_m$	$25.2V_m \cdot I_m$	$Irow_9$	$8.1I_m$	$5V_m$	$40.5V_m \cdot I_m$	$Irow_9$	$8I_m$	$6V_m$	$48V_m \cdot I_m$
$Irow_8$	$6.4I_m$	–	–	$Irow_8$	$8I_m$	$6V_m$	$48V_m \cdot I_m$	$Irow_8$	$7.6I_m$	$8V_m$	$60.8V_m \cdot I_m$	$Irow_8$	$8.4I_m$	$3V_m$	$25.2V_m \cdot I_m$
$Irow_7$	$7.2I_m$	$7V_m$	$50.4V_m \cdot I_m$	$Irow_7$	$7.8I_m$	$8V_m$	$62.4V_m \cdot I_m$	$Irow_7$	$7.6I_m$	–	–	$Irow_7$	$7.8I_m$	$7V_m$	$54.6V_m \cdot I_m$
$Irow_6$	$7.2I_m$	–	–	$Irow_6$	$7.8I_m$	–	–	$Irow_6$	$7.3I_m$	$9V_m$	**$65.7V_m \cdot I_m$**	$Irow_6$	$7.7I_m$	$8V_m$	$61.6V_m \cdot I_m$
$Irow_5$	$9I_m$	$5V_m$	$45V_m \cdot I_m$	$Irow_5$	$8.4I_m$	$3V_m$	$25.2V_m \cdot I_m$	$Irow_5$	$8.1I_m$	$5V_m$	$40.5V_m \cdot I_m$	$Irow_5$	$8.4I_m$	$3V_m$	$25.2V_m \cdot I_m$
$Irow_4$	$9I_m$	–	–	$Irow_4$	$8.3I_m$	$4V_m$	$33.2V_m \cdot I_m$	$Irow_4$	$8.4I_m$	$2V_m$	$16.8V_m \cdot I_m$	$Irow_4$	$8.1I_m$	$4V_m$	$32.4V_m \cdot I_m$
$Irow_3$	$9I_m$	–	–	$Irow_3$	$8I_m$	$6V_m$	$48V_m \cdot I_m$	$Irow_3$	$7.7I_m$	$6V_m$	$46.2V_m \cdot I_m$	$Irow_3$	$8.4I_m$	$3V_m$	$25.2V_m \cdot I_m$
$Irow_2$	$9I_m$	–	–	$Irow_2$	$8.4I_m$	$3V_m$	$25.2V_m \cdot I_m$	$Irow_2$	$8.2I_m$	$3V_m$	$24.6V_m \cdot I_m$	$Irow_2$	$7.4I_m$	$9V_m$	**$66.6V_m \cdot I_m$**
$Irow_1$	$9I_m$	–	–	$Irow_1$	$7.3I_m$	$9V_m$	**$65.7V_m \cdot I_m$**	$Irow_1$	$8.7I_m$	V_m	$8.7V_m \cdot I_m$	$Irow_1$	$8I_m$	$6V_m$	$48V_m \cdot I_m$

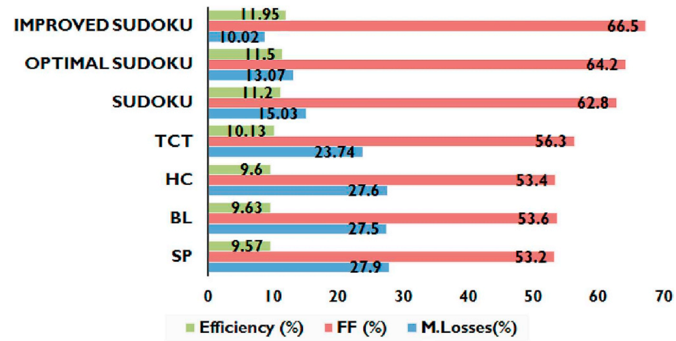

Fig. 21. Mismatch loss, fill factor and efficiency for Group-II shading condition.

irradiance. Remaining four modules, two modules each are receiving 600 W/m^2 and 400 W/m^2 irradiance respectively. The current generated by the *row*6 and *row*7 is,

$$I_{row6} = I_{row7} = 5 \times I_m + 2 \times 0.6I_m + 2 \times 0.4I_m \quad (14)$$

In *row*8 and *row*9, last four PV modules are receiving 600 W/m^2 irradiance and the rest of the modules is receiving 1000 W/m^2 irradiance. The current generated by the *row*8 and *row*9 is,

$$I_{row8} = I_{row9} = 5 \times I_m + 4 \times 0.6I_m \quad (15)$$

Since the current generated by each row is different, there exist multiple peaks in P-V characteristics. Now to find the location of GMPP is a multiplication of voltage and current of the highest peak. The current depends on the amount of irradiance that falls on the PV modules in a row. However, as the voltage across each row is the same (by neglecting voltage drop), the PV array voltage becomes,

$$V_a = 9 \times V_m \quad (16)$$

Power generated by the PV array is,

$$P_a = V_a. I_m = 9V_m. I_m \quad (17)$$

The obtained current, voltage and corresponding power for TCT arrangement is noted in Table 4. The location of GMPP for improved SuDoKu arrangement is calculated as follows.

Location of GMPP for Improved SuDoKu arrangement: Improved SuDoKu arrangement distributes the shading effects over the array under same shading condition, as shown in Fig. 9(c). The current generated by each row is calculated as follows.

In *row*1 and *row*2, only one PV module is receiving 600 W/m^2 irradiance and the rest of the PV modules is receiving 1000 W/m^2 irradiance. The current generated by *row*1 and *row*2 is,

$$I_{row1} = I_{row2} = 8 \times I_m + 0.6I_m \quad (18)$$

In *row*3, *row*4 and *row*7, two PV modules are receiving 600 W/m^2 irradiance and the rest of the PV modules is receiving 1000 W/m^2 irradiance. The current generated by *row*3, *row*4 and *row*7 is,

$$I_{row3} = I_{row4} = I_{row7} = 7 \times I_m + 2 \times 0.6I_m \quad (19)$$

In *row*5, *row*6, *row*8 and *row*9, two PV modules are receiving different irradiances such as 600 W/m^2 and 400 W/m^2 respectively. The rest of the modules is receiving 1000 W/m^2 irradiance. The current generated by these rows,

$$I_{row5} = I_{row6} = I_{row8} = I_{row9} = 7 \times I_m + 0.6I_m + 0.4I_m \quad (20)$$

The obtained current, voltage and corresponding power for improved SuDoKu arrangement is noted in Table 4. Similarly, the location of GMPP for SuDoKu [41] and optimal SuDoKu [42] arrangements are calculated theoretically under the same shading condition and are presented in Table 4. From the table, it is observed that the highest GMPP 72 V_m. I_m is produced by the improved SuDoKu arrangement as

Table 6
Location of GMPP for TCT, SuDoKu [41], Optimal SuDoKu [42] and Improved SuDoKu PV array arrangements under group-III shading condition.

TCT arrangement				SuDoKu arrangement [41]				Optimal SuDoKu arrangement [42]				Improved SuDoKu arrangement			
Row bypassed	currents (I_a)	voltages (V_a)	power (P_a)	Row bypassed	currents (I_a)	voltages (V_a)	power (P_a)	Row bypassed	currents (I_a)	voltages (V_a)	power (P_a)	Row bypassed	currents (I_a)	voltages (V_a)	power (P_a)
$Irow_9$	$9I_m$	$5V_m$	$45V_m \cdot I_m$	$Irow_9$	$7.4I_m$	$8V_m$	$59.2V_m \cdot I_m$	$Irow_9$	$8.2I_m$	$2V_m$	$16.4V_m \cdot I_m$	$Irow_9$	$7.2I_m$	$9V_m$	**$64.8V_m \cdot I_m$**
$Irow_8$	$9I_m$	–	–	$Irow_8$	$8.2I_m$	$5V_m$	$41V_m \cdot I_m$	$Irow_8$	$7.1I_m$	$9V_m$	**$63.9V_m \cdot I_m$**	$Irow_8$	$7.6I_m$	$7V_m$	$53.2V_m \cdot I_m$
$Irow_7$	$9I_m$	–	–	$Irow_7$	$6.8I_m$	$9V_m$	**$61.2V_m \cdot I_m$**	$Irow_7$	$8I_m$	$3V_m$	$24V_m \cdot I_m$	$Irow_7$	$7.6I_m$	$7V_m$	$53.2V_m \cdot I_m$
$Irow_6$	$9I_m$	–	–	$Irow_6$	$8.2I_m$	$5V_m$	$41V_m \cdot I_m$	$Irow_6$	$7.8I_m$	$6V_m$	$46.8V_m \cdot I_m$	$Irow_6$	$7.6I_m$	–	–
$Irow_5$	$9I_m$	–	–	$Irow_5$	$8.2I_m$	$5V_m$	$41V_m \cdot I_m$	$Irow_5$	$7.1I_m$	$9V_m$	$63.9V_m \cdot I_m$	$Irow_5$	$8.6I_m$	$2V_m$	$17.2V_m \cdot I_m$
$Irow_4$	$6.2I_m$	$9V_m$	**$55.8V_m \cdot I_m$**	$Irow_4$	$8.6I_m$	$2V_m$	$17.2V_m \cdot I_m$	$Irow_4$	$7.1I_m$	–	–	$Irow_4$	$8.6I_m$	$2V_m$	$17.2V_m \cdot I_m$
$Irow_3$	$6.2I_m$	–	–	$Irow_3$	$8.6I_m$	–	–	$Irow_3$	$7.8I_m$	$6V_m$	$46.8V_m \cdot I_m$	$Irow_3$	$7.6I_m$	$7V_m$	$53.2V_m \cdot I_m$
$Irow_2$	$6.6I_m$	$7V_m$	$46.2V_m \cdot I_m$	$Irow_2$	$7.8I_m$	$7V_m$	$54.6V_m \cdot I_m$	$Irow_2$	$7.8I_m$	–	–	$Irow_2$	$7.4I_m$	$8V_m$	$59.2V_m \cdot I_m$
$Irow_1$	$6.6I_m$	–	–	$Irow_1$	$7.8I_m$	–	–	$Irow_1$	$8.2I_m$	$2V_m$	$16.4V_m \cdot I_m$	$Irow_1$	$7.8I_m$	$3V_m$	$23.4V_m \cdot I_m$

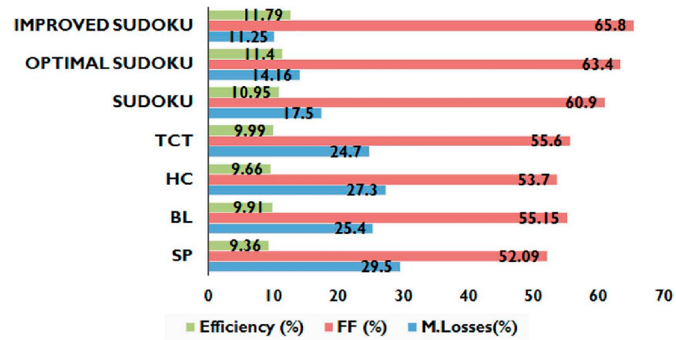

Fig. 22. Mismatch loss, fill factor and efficiency for Group-III shading condition.

compared to TCT, SuDoKu and optimal SuDoKu PV array arrangements. The theoretical GMPP validated by plotting the simulated I-V and P-V characteristics is shown in Fig. 10. In addition, SP, BL and HC PV array configurations also simulated under the same shading condition is shown in Fig. 10. Under this condition, the obtained parameters such as GMPP, ML (%), FF(%) and η(%) for all configurations are graphically represented in Figs. 19 and 20. From the figures, it is noticed that the improved SuDoKu arrangement enhances the global maximum power by 15.3%, 13.9%, 11.13%, 9.67%, 2.8%, and 2.3% as compared to SP, BL, HC, TCT, SuDoKu and optimal SuDoKu PV array configurations.

Group-II Shading: In group-II, the bottom of left corner 4 × 4 sub-array matrix is subjected to partial shading with various irradiance levels as shown in Fig. 11(a).

Location of GMPP for TCT arrangement: In *row*1 to *row*5, all PV modules are receiving uniform irradiance 1000 W/m^2 is shown in Fig. 11(a). The current generated by these rows,

$$I_{row1} = I_{row2} = I_{row3} = I_{row4} = I_{row5} = 9 \times I_m \tag{21}$$

In *row*6 and *row*7, first four PV modules, each two are receiving 400 W/m^2 and 700 W/m^2 irradiance respectively, the rest of the PV modules is receiving 1000 W/m^2 irradiance. The current generated by the *row*6 and *row*7 is,

$$I_{row6} = I_{row7} = 5 \times I_m + 2 \times 0.4I_m + 2 \times 0.7I_m \tag{22}$$

In *row*8 and *row*9, first four modules, each two are receiving 400 W/m^2 and 300 W/m^2 irradiance respectively, the rest of the PV modules is receiving 1000 W/m^2 irradiance. The current generated by the *row*8 and *row*9 is,

$$I_{row8} = I_{row9} = 5 \times I_m + 2 \times 0.4I_m + 2 \times 0.3I_m \tag{23}$$

The obtained current, voltage and corresponding power for TCT arrangement is noted in Table 5.

Location of GMPP for Improved SuDoKu arrangement: Improved SuDoKu arrangement distributes the shading effects over the array under same shading condition, as shown in Fig. 11(c). The current generated by each row is calculated as follows.

In *row*1 and *row*9, only two PV modules are receiving individual irradiance such as 700 W/m^2 and 300 W/m^2, the rest of the PV modules is receiving 1000 W/m^2 irradiance. The current generated by *row*1 and *row*9 is,

$$I_{row1} = I_{row9} = 7 \times I_m + 0.7I_m + 0.3I_m \tag{24}$$

Similarly, the current generated by *row*2 is,

$$I_{row2} = 6 \times I_m + 0.4I_m + 0.7I_m + 0.3I_m \tag{25}$$

The current generated by *row*3, *row*5 and *row*8,

$$I_{row3} = I_{row5} = I_{row8} = 8 \times I_m + 0.4I_m \tag{26}$$

The current generated by *row*4 is,

Table 7
Location of GMPP for TCT, SuDoKu [41], Optimal SuDoKu [42] and Improved SuDoKu PV array arrangements under group-IV shading condition.

TCT arrangement				SuDoKu arrangement [41]				Optimal SuDoKu arrangement [42]				Improved SuDoKu arrangement			
Row bypassed	currents (I_a)	voltages (V_a)	power (P_a)	Row bypassed	currents (I_a)	voltages (V_a)	power (P_a)	Row bypassed	currents (I_a)	voltages (V_a)	power (P_a)	Row bypassed	currents (I_a)	voltages (V_a)	power (P_a))
$Irow_9$	$9I_m$	$5V_m$	$45V_m \cdot I_m$	$Irow_9$	$7.6I_m$	$6V_m$	$45.6V_m \cdot I_m$	$Irow_9$	$8.7I_m$	V_m	$8.7V_m \cdot I_m$	$Irow_9$	$7.4I_m$	$8V_m$	$59.2V_m \cdot I_m$
$Irow_8$	$9I_m$	–	–	$Irow_8$	$7.7I_m$	$5V_m$	$38.5V_m \cdot I_m$	$Irow_8$	$8.1I_m$	$4V_m$	$32.4V_m \cdot I_m$	$Irow_8$	$7.8I_m$	$4V_m$	$31.2V_m \cdot I_m$
$Irow_7$	$9I_m$	–	–	$Irow_7$	$8.5I_m$	V_m	$8.5V_m \cdot I_m$	$Irow_7$	$7.4I_m$	$8V_m$	$59.2V_m \cdot I_m$	$Irow_7$	$8.5I_m$	$2V_m$	$17V_m \cdot I_m$
$Irow_6$	$9I_m$	–	–	$Irow_6$	$8.3I_m$	$2V_m$	$16.6V_m \cdot I_m$	$Irow_6$	$8.3I_m$	$3V_m$	$24.9V_m \cdot I_m$	$Irow_6$	$8.5I_m$	–	–
$Irow_5$	$9I_m$	–	–	$Irow_5$	$7.8I_m$	$4V_m$	$31.2V_m \cdot I_m$	$Irow_5$	$8.5I_m$	$2V_m$	$17V_m \cdot I_m$	$Irow_5$	$6.7I_m$	$9V_m$	**$60.3V_m \cdot I_m$**
$Irow_4$	$6I_m$	$9V_m$	**$54V_m \cdot I_m$**	$Irow_4$	$6.6I_m$	$9V_m$	**$59.4V_m \cdot I_m$**	$Irow_4$	$7.7I_m$	$5V_m$	$38.5V_m \cdot I_m$	$Irow_4$	$7.4I_m$	$8V_m$	$59.2V_m \cdot I_m$
$Irow_3$	$6I_m$	–	–	$Irow_3$	$7.4I_m$	$8V_m$	$59.2V_m \cdot I_m$	$Irow_3$	$7.5I_m$	$6V_m$	$45V_m \cdot I_m$	$Irow_3$	$7.6I_m$	$5V_m$	$38V_m \cdot I_m$
$Irow_2$	$6.2I_m$	$7V_m$	$43.4V_m \cdot I_m$	$Irow_2$	$8.1I_m$	$3V_m$	$24.3V_m \cdot I_m$	$Irow_2$	$7.4I_m$	$8V_m$	$59.2V_m \cdot I_m$	$Irow_2$	$8.1I_m$	$3V_m$	$24.3V_m \cdot I_m$
$Irow_1$	$6.2I_m$	–	–	$Irow_1$	$7.4I_m$	$8V_m$	$59.2V_m \cdot I_m$	$Irow_1$	$6.6I_m$	$9V_m$	**$59.4V_m \cdot I_m$**	$Irow_1$	$7.4I_m$	$8V_m$	$59.2V_m \cdot I_m$

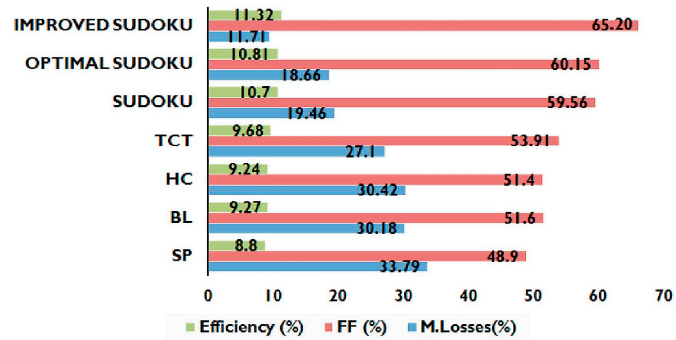

Fig. 23. Mismatch loss, fill factor and efficiency for Group-IV shading condition.

$$I_{row4} = 7 \times I_m + 0.7I_m + 0.4I_m \tag{27}$$

The current generated by $row6$ and $row7$,

$$I_{row6} = 7 \times I_m + 0.4I_m + 0.3I_m \tag{28}$$

$$I_{row7} = 7 \times I_m + 2 \times 0.4I_m \tag{29}$$

The obtained current, voltage and corresponding power for Improved SuDoKu arrangement is noted in Table 5. Similarly, the location of GMPP for SuDoKu [41], optimal SuDoKu [42] arrangements are calculated theoretically under the same shading condition and are presented in Table 5. From the table, it is clearly observed that the highest GMPP $66.6V_m \cdot I_m$ is produced by the improved SuDoKu arrangement as compared to TCT, SuDoKu and optimal SuDoKu PV array arrangements. The theoretical GMPP validated by plotting the simulated I-V and P-V characteristics is shown in Fig. 12. In addition, SP, BL and HC PV array configurations also simulated under the same shading condition is shown in Fig. 12. Under this condition, the obtained parameters such as GMPP, ML (%), FF(%) and η(%) for all PV array configurations are graphically represented in Figs. 19 and 21. From the figures, it is noticed that the improved SuDoKu arrangement enhances the global maximum power by 24.9%, 24.1%, 24.6%, 19.2%, 6.9% and 4.4% as compared to SP, BL, HC, TCT, SuDoKu and optimal SuDoKu PV array configurations.

The same procedure is applied to other shading conditions to find the location of GMPP.

Group-III Shading: In group-III, the top most right corner 4 × 4sub-array matrix is subjected to partial shading with different irradiance levels as shown in Fig. 13(a). The location of GMPP for TCT, SuDoKu [38], optimal SuDoKu [42], and improved SuDoKu arrangements are calculated theoretically and are presented in Table 6. From the table, it is observed that the highest GMPP $64.8V_m \cdot I_m$ is produced by the improved SuDoKu arrangement as compared to TCT, SuDoKu and optimal SuDoKu arrangements. The theoretical GMPP validated by plotting the simulated I-V and P-V characteristics is shown in Fig. 14. In addition, SP, BL and HC PV array configurations also simulated under the same shading condition is shown in Fig. 14. Under this condition, the obtained parameters such as GMPP, ML (%), FF(%) and η(%) for all PV array configurations are graphically represented in Figs. 19 and 22. From the figures, it is noticed that the improved SuDoKu arrangement enhances the global maximum power by 25.7%, 19.3%, 22.3%, 18.5%, 8.8% and 4.2% as compared to SP, BL, HC, TCT, SuDoKu and optimal SuDoKu PV array configurations.

Group-IV Shading: Group-IV, the top most left corner 4 × 4sub-array matrix is subjected to partial shading with different irradiance levels as shown in Fig. 15(a). The location of GMPP for TCT, SuDoKu, optimal SuDoKu, and improved SuDoKu arrangements are calculated theoretically and are presented in Table 7. From the table, it is observed that the highest GMPP $60.3V_m \cdot I_m$ is produced by the improved SuDoKu

Table 8
Location of GMPP for TCT, SuDoKu [41], Optimal SuDoKu [42] and Improved SuDoKu PV array arrangements under group-V shading condition.

TCT arrangement				SuDoKu arrangement [41]				Optimal SuDoKu arrangement [42]				Improved SuDoKu arrangement			
Row bypassed	currents (I_a)	voltages (V_a)	power (..)	Row bypassed	currents (I_a)	voltages (V_a)	power (P_a)	Row bypassed	currents (I_a)	voltages (V_a)	power (P_a)	Row bypassed	currents (I_a)	voltages (V_a)	power (P_a)
$Irow_9$	$9I_m$	$5V_m$	$45V_m \cdot I_m$	$Irow_9$	$7.4I_m$	$9V_m$	$\mathbf{66.9}V_m \cdot I_m$	$Irow_9$	$8.4I_m$	$2V_m$	$16.8V_m \cdot I_m$	$Irow_9$	$8.3I_m$	$2V_m$	$16.6V_m \cdot I_m$
$Irow_8$	$9I_m$	–	–	$Irow_8$	$8.4I_m$	$2V_m$	$16.8V_m \cdot I_m$	$Irow_8$	$8I_m$	$5V_m$	$40V_m \cdot I_m$	$Irow_8$	$8.3I_m$	–	–
$Irow_7$	$9I_m$	–	–	$Irow_7$	$7.5I_m$	$8V_m$	$60V_m \cdot I_m$	$Irow_7$	$8.6I_m$	V_m	$8.6V_m \cdot I_m$	$Irow_7$	$7.5I_m$	$9V_m$	$\mathbf{67.5}V_m \cdot I_m$
$Irow_6$	$6.8I_m$	$7V_m$	$47.6V_m \cdot I_m$	$Irow_6$	$8.3I_m$	$4V_m$	$33.2V_m \cdot I_m$	$Irow_6$	$8.2I_m$	$3V_m$	$24.9V_m \cdot I_m$	$Irow_6$	$8.2I_m$	$3V_m$	$24.6V_m \cdot I_m$
$Irow_5$	$6.8I_m$	–	–	$Irow_5$	$7.8I_m$	$6V_m$	$46.8V_m \cdot I_m$	$Irow_5$	$7.5I_m$	$8V_m$	$60V_m \cdot I_m$	$Irow_5$	$7.6I_m$	$8V_m$	$60.8V_m \cdot I_m$
$Irow_4$	$6.2I_m$	$9V_m$	$\mathbf{55.8}V_m \cdot I_m$	$Irow_4$	$7.6I_m$	$7V_m$	$53.2V_m \cdot I_m$	$Irow_4$	$7.9I_m$	$6V_m$	$47.4V_m \cdot I_m$	$Irow_4$	$7.8I_m$	$6V_m$	$46.8V_m \cdot I_m$
$Irow_3$	$6.2I_m$	–	–	$Irow_3$	$8.6I_m$	V_m	$8.6V_m \cdot I_m$	$Irow_3$	$8I_m$	$5V_m$	$40V_m \cdot I_m$	$Irow_3$	$7.8I_m$	–	–
$Irow_2$	$9I_m$	$5V_m$	$45V_m \cdot I_m$	$Irow_2$	$8.3I_m$	$4V_m$	$33.2V_m \cdot I_m$	$Irow_2$	$6.9I_m$	$9V_m$	$\mathbf{62.1}V_m \cdot I_m$	$Irow_2$	$7.6I_m$	$8V_m$	$60.8V_m \cdot I_m$
$Irow_1$	$9I_m$	–	–	$Irow_1$	$7.8I_m$	$6V_m$	$46.8V_m \cdot I_m$	$Irow_1$	$7.5I_m$	$8V_m$	$60V_m \cdot I_m$	$Irow_1$	$7.9I_m$	$4V_m$	$31.6V_m \cdot I_m$

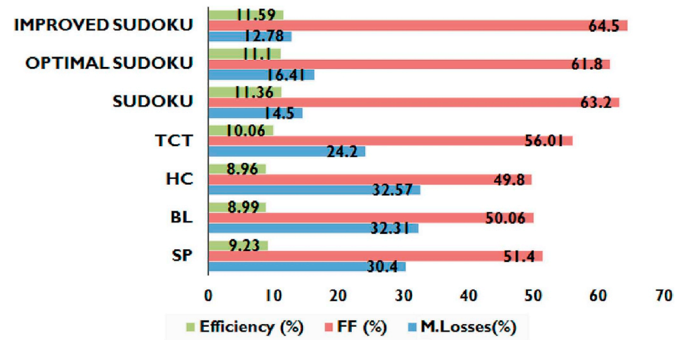

Fig. 24. Mismatch loss, fill factor and efficiency for Group-V shading condition.

arrangement as compared to TCT, SuDoKu and optimal SuDoKu PV array arrangements. The theoretical GMPP validated by plotting the simulated I-V and P-V characteristics is shown in Fig. 16. In addition, SP, BL and HC PV array configurations also simulated under the same shading condition is shown in Fig. 16. Under this condition, the obtained parameters such as GMPP, ML (%), FF(%) and η(%) for all PV array configurations are graphically represented in Figs. 19 and 23. From the figures, it is noticed that the improved SuDoKu arrangement enhances the global maximum power by 28.6%, 22.1%, 22.8%, 17.2%, 6.2% and 5.2% as compared to SP, BL, HC, TCT, SuDoKu and optimal SuDoKu PV array configurations.

Group-V Shading: In group-V, the 4 × 4sub-array matrix is subjected to partial shading at the center with various irradiance levels as shown in Fig. 17(a). The location of GMPP for TCT, SuDoKu, optimal SuDoKu, and improved SuDoKu arrangements are calculated theoretically and are presented in Table 8. From the table, it is observed that the highest GMPP $67.5V_m.\ I_m$ is produced by the improved SuDoKu arrangement as compared to TCT, SuDoKu and optimal SuDoKu PV array arrangements. The theoretical GMPP validated by plotting the simulated I-V and P-V characteristics is shown in Fig. 18. In addition, SP, BL and HC PV array configurations also simulated under the same shading condition is shown in Fig. 18. Under this condition, the obtained parameters such as GMPP, ML (%), FF(%) and η(%) for all PV array configurations are graphically represented in Figs. 19 and 24. From the figures, it is noticed that the improved SuDoKu arrangement enhances the global maximum power by 26.9%, 30.3%, 30.8%, 16.8%, 4.2%, and 6.3% as compared to SP, BL, HC, TCT, SuDoKu and optimal SuDoKu PV array configurations.

From the studies mentioned above, it is inferred that the improved SuDoKu arrangement is enhancing the global maximum power as compared to SP, TCT, BL, HC, SuDoKu [41] and optimal SuDoKu [42] PV array configurations under all shading conditions.

5. Conclusion

This paper proposed an improved SuDoKu arrangement for TCT PV array to increase maximum power output under partial shading conditions. In this paper, five important shading conditions are considered. In each condition, the location of GMPP is calculated and validated by using MATLAB/SIMULINK. Also, the performance of the proposed arrangement is investigated along with SP, TCT, BL, HC, SuDoKu and optimal SuDoKu PV array configurations by comparing the GMPP, mismatch losses, fill factor and efficiency. From the results mentioned above, it is clearly observed that the improved SuDoKu arrangement enhances the global maximum power and reduces the mismatch losses as compared to SP, TCT, BL, HC, SuDoKu and optimal SuDoKu PV array configurations under all shading conditions. Moreover, the proposed arrangement defeated the multiple peaks under most shading conditions.

Appendix A. Supplementary data

Supplementary data to this article can be found online at https://doi.org/10.1016/j.rser.2019.04.037.

References

[1] Sahoo SK. Renewable and sustainable energy reviews solar photovoltaic energy progress in India: a review. Renew Sustain Energy Rev 2016;59:927–39.

[2] Li G, Xuan Q, Pei G, Su Y, Ji J. Effect of non-uniform illumination and temperature distribution on concentrating solar cell-a review. Energy 2018;144:1119–36.

[3] Mellit A, Tina GM, Kalogirou SA. Fault detection and diagnosis methods for photovoltaic systems: a review. Renew Sustain Energy Rev 2018;91:1–17.

[4] Patel H, Agarwal V. Matlab-based modeling to study the effects of partial shading on pv array characteristics. IEEE Trans Energy Convers 2008;23(1):302–10.

[5] Bernardini A, Sarti A, Maffezzoni P, Daniel L. Wave digital-based variability analysis of electrical mismatch in photovoltaic arrays. Circuits and systems (ISCAS), 2018 IEEE international symposium on. IEEE; 2018. p. 1–5.

[6] Li G, Jin Y, Akram M, Chen X, Ji J. Application of bio-inspired algorithms in maximum power point tracking for pv systems under partial shading conditions–a review. Renew Sustain Energy Rev 2018;81:840–73.

[7] Jin Y, Hou W, Li G, Chen X. A glowworm swarm optimization-based maximum power point tracking for photovoltaic/thermal systems under non-uniform solar irradiation and temperature distribution. Energies 2017;10(4):541.

[8] Wang Y-J, Hsu P-C. An investigation on partial shading of pv modules with different connection configurations of pv cells. Energy 2011;36(5):3069–78.

[9] Pendem SR, Mikkili S. Modeling, simulation and performance analysis of solar pv array configurations (series, series–parallel and honey-comb) to extract maximum power under partial shading conditions. Energy Rep 2018;4:274–87.

[10] Gautam NK, Kaushika N. Reliability evaluation of solar photovoltaic arrays. Sol Energy 2002;72(2):129–41.

[11] Bingöl O, Özkaya B. Analysis and comparison of different pv array configurations under partial shading conditions. Sol Energy 2018;160:336–43.

[12] Pendem SR, Mikkili S. Modelling and performance assessment of pv array topologies under partial shading conditions to mitigate the mismatching power losses. Sol Energy 2018;160:303–21.

[13] Laudani A, Lozito GM, Lucaferri V, Radicioni M, Fulginei FR. On circuital topologies and reconfiguration strategies for pv systems in partial shading conditions: a review. AIMS Energy 2018;6(5):735–63.

[14] La Manna D, Vigni VL, Sanseverino ER, Di Dio V, Romano P. Reconfigurable electrical interconnection strategies for photovoltaic arrays: a review. Renew Sustain Energy Rev 2014;33:412–26.

[15] G. Petrone, G. Spagnuolo, Y. Zhao, B. Lehman, C. Ramos, M. Orozco, Dynamical reconfiguration for fighting mismatched conditions and meeting load requests.

[16] Salameh ZM, Dagher F. The effect of electrical array reconfiguration on the performance of a pv-powered volumetric water pump. IEEE Trans Energy Convers 1990;5(4):653–8.

[17] Salameh ZM, Liang C. Optimum switching points for array reconfiguration controller. 1990. p. 971–6.

[18] Auttawaitkul Y, Pungsiri B, Chammongthai K, Okuda M. A method of appropriate electrical array reconfiguration management for photovoltaic powered car. 1998. p. 201–4.

[19] Velasco-Quesada G, Guinjoan-Gispert F, Piqué-López R, Román-Lumbreras M, Conesa-Roca A. Electrical pv array reconfiguration strategy for energy extraction improvement in grid-connected pv systems. IEEE Trans Ind Electron 2009;56(11):4319–31.

[20] Velasco G, Guinjoan F, Pique R. Grid-connected pv systems energy extraction improvement by means of an electric array reconfiguration (ear) strategy: operating principle and experimental results. 2008. p. 1983–8.

[21] El-Dein MS, Kazerani M, Salama M. Optimal photovoltaic array reconfiguration to reduce partial shading losses. IEEE Trans Sustain Energy 2013;4(1):145–53.

[22] Nguyen D, Lehman B. An adaptive solar photovoltaic array using model-based reconfiguration algorithm. IEEE Trans Ind Electron 2008;55(7):2644–54.

[23] Nguyen D, Lehman B. A reconfigurable solar photovoltaic array under shadow conditions. 2008. p. 980–6.

[24] Parlak KŞ. Pv array reconfiguration method under partial shading conditions. Int J Electr Power Energy Syst 2014;63:713–21.

[25] Krishna GS, Moger T. Reconfiguration strategies for reducing partial shading effects in photovoltaic arrays: state of the art. Sol Energy 2019;182:429–52https://doi.org/10.1016/j.solener.2019.02.057http://www.sciencedirect.com/science/article/pii/S0038092X19301835.

[26] Romano P, Candela R, Cardinale M, Li Vigni V, Musso D, Riva Sanseverino E. Optimization of photovoltaic energy production through an efficient switching matrix. J Sustain Dev Energy, Water, Environ Syst 2013;1(3):227–36.

[27] Storey JP, Wilson PR, Bagnall D. Improved optimization strategy for irradiance equalization in dynamic photovoltaic arrays. IEEE Trans Power Electron 2013;28(6):2946–56.

[28] Matam M, Barry VR. Variable size dynamic pv array for small and various dc loads. Sol Energy 2018;163:581–90.

[29] Karakose M, Baygin M, Parlak KS. A new real-time reconfiguration approach based on neural network in partial shading for pv arrays. 2014. p. 633–7.

[30] Karakose M, Baygin M. Image processing based analysis of moving shadow effects for reconfiguration in pv arrays. 2014. p. 683–7.

[31] Tabanjat A, Becherif M, Hissel D. Reconfiguration solution for shaded pv panels using switching control. Renew Energy 2015;82:4–13.

[32] Karakose M, Baygin M, Murat K, Baygin N, Akin E. Fuzzy based reconfiguration method using intelligent partial shadow detection in pv arrays. Int J Comput Intell Syst 2016;9(2):202–12.

[33] Sanseverino ER, Ngoc TN, Cardinale M, Vigni VL, Musso D, Romano P, Viola F. Dynamic programming and munkres algorithm for optimal photovoltaic arrays reconfiguration. Sol Energy 2015;122:347–58.

[34] Ngoc TN, Phung QN, Tung LN, Sanseverino ER, Romano P, Viola F. Increasing efficiency of photovoltaic systems under non-homogeneous solar irradiation using improved dynamic programming methods. Sol Energy 2017;150:325–34.

[35] Jazayeri M, Jazayeri K, Uysal S. Adaptive photovoltaic array reconfiguration based on real cloud patterns to mitigate effects of non-uniform spatial irradiance profiles. Sol Energy 2017;155:506–16.

[36] Mahmoud Y, El-Saadany EF. Enhanced reconfiguration method for reducing mismatch losses in pv systems. IEEE J Photovoltaics 2017;7(6):1746–54.

[37] Ramasamy S, Seenithangam J, Dash SS, Chaitanya K. A dodging algorithm to reconfigure photovoltaic array to negate partial shading effect. Prog Photovoltaics Res Appl 2016;24(2):200–10.

[38] Rao PS, Ilango GS, Nagamani C. Maximum power from pv arrays using a fixed configuration under different shading conditions. IEEE J Photovoltaics 2014;4(2):679–86.

[39] Yadav AS, Pachauri RK, Chauhan YK, Choudhury S, Singh R. Performance enhancement of partially shaded pv array using novel shade dispersion effect on magic-square puzzle configuration. Sol Energy 2017;144:780–97.

[40] Yadav AS, Pachauri RK, Chauhan YK. Comprehensive investigation of pv arrays with puzzle shade dispersion for improved performance. Sol Energy 2016;129:256–85.

[41] Rani BI, Ilango GS, Nagamani C. Enhanced power generation from pv array under partial shading conditions by shade dispersion using su do ku configuration. IEEE Trans Sustain Energy 2013;4(3):594–601.

[42] Potnuru SR, Pattabiraman D, Ganesan SI, Chilakapati N. Positioning of pv panels for reduction in line losses and mismatch losses in pv array. Renew Energy 2015;78:264–75.

[43] Sahu HS, Nayak SK, Mishra S. Maximizing the power generation of a partially shaded pv array. IEEE J Emerg Sel Top Power Electron 2016;4(2):626–37.

[44] Pachauri R, Yadav AS, Chauhan YK, Sharma A, Kumar V. Shade dispersion-based photovoltaic array configurations for performance enhancement under partial shading conditions. Int Trans Electr Energy Syst 2018;28.

[45] Horoufiany M, Ghandehari R. Optimization of the sudoku based reconfiguration technique for pv arrays power enhancement under mutual shading conditions. Sol Energy 2018;159:1037–46.

[46] Malathy S, Ramaprabha R. A static pv array architecture to enhance power generation under partial shaded conditions. 2015. p. 341–6.

[47] Satpathy PR, Sharma R, Jena S. A shade dispersion interconnection scheme for partially shaded modules in a solar pv array network. Energy 2017;139:350–65.

[48] Vijayalekshmy S, Bindu G, Iyer SR. A novel zig-zag scheme for power enhancement of partially shaded solar arrays. Sol Energy 2016;135:92–102.

[49] Belhaouas N, Cheikh M-SA, Agathoklis P, Oularbi M-R, Amrouche B, Sedraoui K, Djilali N. Pv array power output maximization under partial shading using new shifted pv array arrangements. Appl Energy 2017;187:326–37.

[50] Dhanalakshmi B, Rajasekar N. Dominance square based array reconfiguration scheme for power loss reduction in solar photovoltaic (pv) systems. Energy Convers Manag 2018;156:84–102.

[51] Gonzalez Montoya D, Bastidas-Rodriguez JD, Trejos-Grisales LA, Ramos-Paja CA, Petrone G, Spagnuolo G. A procedure for modeling photovoltaic arrays under any configuration and shading conditions. Energies 2018;11(4):767.

[52] Jena D, Ramana VV. Modeling of photovoltaic system for uniform and non-uniform irradiance: a critical review. Renew Sustain Energy Rev 2015;52:400–17.

[53] Bernardini A, Maffezzoni P, Daniel L, Sarti A. Wave-based analysis of large nonlinear photovoltaic arrays. IEEE Trans Circuits Syst I: Regul Pap 2018;65(4):1363–76.

[54] Tian H, Mancilla-David F, Ellis K, Muljadi E, Jenkins P. A cell-to-module-to-array detailed model for photovoltaic panels. Sol Energy 2012;86(9):2695–706.